FERMILAB-PUB-10-428-E

# Double parton interactions as a background to associated $HW$ production at the Tevatron

Dmitry Bandurin[1], Georgy Golovanov[2], Nikolai Skachkov[2]

[1] *Department of Physics, Florida State University, Tallahassee, FL 32306*
[2] *Joint Institute for Nuclear Research, Dubna, Russia, Joliot-Curie 6, 141980*

**Abstract**

In this paper we study events with $W$+jets final state, produced in double parton (DP) interactions, as a background to the associated Higgs boson ($H$) and $W$ production, with $H \to b\bar{b}$ decay, at the Tevatron. We have found that the event yield from the DP background can be quite sizable, what necessitates a choice of selection criteria to separate the $HW$ and DP production processes. We suggest a set of variables sensitive to the kinematics of DP and $HW$ events. We show that these variables, being used as an input to the artificial neural network, allow one to significantly improve a sensitivity to the Higgs boson production.

## I. INTRODUCTION

A significant amount of experimental data, ranging from ISR energies [1] through the SPS [2, 3] to the Tevatron [4–8], and even to photoproduction at HERA [9, 10], shows a clear evidence of hard jets produced due to multiple parton interactions (MPI). Specifically, in the Tevatron Run I and Run II studies, 4-jet [4] and $\gamma + 3$-jet events [5, 8] have been considered with jet $p_T \gtrsim 5-15$ GeV and fraction of events occurring due to double parton (DP) interactions have been measured. Those fractions varied depending on the final state and the jet transverse momentum $p_T$ in the second parton interaction. The fraction measured using 4-jet final state is found to be 5.5% for jet $p_T > 25$ GeV [4]. The fractions obtained from the $\gamma + 3$-jet production range from 51.3% for the second (ordered in $pT$) and third jet $p_T$ in the interval $5 - 7$ GeV[1] [5] to $47\% - 22\%$ for the second jet $p_T$ within $15 - 30$ GeV [8].

Those experiments have also measured effective cross section $\sigma_{\rm eff}$, an important parameter that contains information about the parton spatial density inside the (anti)proton: $\sigma_{\rm eff} = 12.1^{+10.7}_{-5.4}$ mb in the 4-jet production in CDF [4], $\sigma_{\rm eff} = 14.5 \pm 1.7^{+1.7}_{-2.3}$ mb and $\sigma_{\rm eff} = 16.4 \pm 0.3 \pm 2.3$ mb in the $\gamma$+3-jet productions in CDF [5] and D0 [8], correspondingly. This parameter allows one to calculate a DP cross section $\sigma_{DP}$ for any pair of partonic processes $A$ and $B$ according to:

$$\sigma_{DP} \equiv m \frac{\sigma^A \sigma^B}{\sigma_{\rm eff}}. \quad (1)$$

The factor $m$ has a Poissonian nature [11] and should be equal to 1/2 for two indistinguishable processes (like two dijet productions in $A$ and $B$) or gives unity for the distinguishable ones. The CDF [5] and D0 [8] experiments obtained most accurate results on $\sigma_{\rm eff}$ which led to an average value of about $\sigma^{\rm ave}_{\rm eff} = 15.5$ mb.

In addition to information about parton spatial structure, those studies also pointed out that the DP interactions can be a noticeable background to many rare processes, especially for those with multijet final state. In this case an additional partonic interaction, with most probable dijet final state, can mimic the multijet signal signature. Some estimates of the DP background to the Higgs boson production processes at the LHC have been done in [12–14].

In this paper we consider the DP events, caused by the $W$+dijet production, as a background to the $HW$ production, with $W \to l\nu$ and $H \to b\bar{b}$ decays, which is one of the most promising Higgs boson search channels at the Tevatron. An example of a possible DP process with $W + b\bar{b}$ production is shown in Fig. 1. However, in addition to the two-$b$-jet final state produced in the second parton scattering, we should also expect quite significant contribution from final states with light+heavy flavor and two light jets.

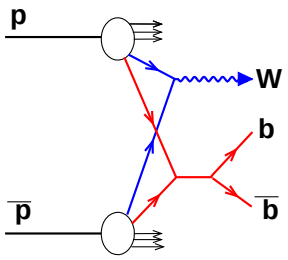


Figure 1: A possible diagram for $W + b\bar{b}$ production due to DP scattering.

Due to a similarity of $HW$ and $HZ$ final states, we expect that a relative DP background from $Z$+dijet production to the $HZ$ events should be quite close to the $HW$ case. For this reason, we limited our consideration in the paper by the $HW$ events only (and relevant DP background to them).

This paper is organized as follows. In Section II we describe the way how the DP and Higgs boson samples are simulated and selected. In Section III we calculate differential cross sections $d\sigma/dM_{jj}$ (where $M_{jj}$ is the invariant mass of the two leading jets) and event yields in the $HW$ and DP processes with account of jet energy detector smearing and $b$-jet identification effects. The rates of events with $W$+2-jet production due to the DP and conventional single parton (SP) scatterings are compared in Section IV. In Section V we introduce a set of variables sensitive to the kinematics of the signal $HW(Z)$ and DP background final states and use them as an input to a dedicated Artificial Neural Network (ANN) to separate the two event types. We make our conclusions in Section VI.

[1] In this measurement jet $p_T$ is raw, i.e. uncorrected for the energy losses [5].

## II. SIMULATION AND SELECTIONS

### A. Selections

Nowadays PYTHIA event generator [15] is the best framework to study many effects related to MPI production. It includes a few sophisticated phenomenological models which consider the MPI scatterings with their various correlations, including parton momentum and color. The MPI models in PYTHIA 6, being tuned to experimental results, reproduce many observables in data quite well [11, 16]. PYTHIA 8, which inherited most features from its precessor, in addition allows to combine a variety of different kinds of parton processes in the first (main) and second scatterings within kinematic regions of interest. To simulate events for the study we used PYTHIA 8 with Tune 2C as an MPI model [17]. The $HW$ production channel simulated with the Higgs boson masses $m_H = 115$ and 150 GeV was considered. Background events from the DP scattering were simulated as the inclusive $q\bar{q} \to W + X$ production in the first parton process and inclusive QCD dijet production in the second process. To increase statistics in the selected final states with the cuts above, the $W$ scattering process is required to have invariant mass $50 < m_W < 120$ GeV and a minimal allowed parton transverse momentum $\hat{p}_\perp^{min}$ in the dijet process is required to be $\hat{p}_\perp^{min} = 10$ GeV.

The event selection criteria are taken from [18] and applied to both, the $HW$ and DP production events and briefly summarized below:

• Higgs boson is required to decay into $b\bar{b}$.

• W-boson is selected in the electron and muon decay modes with lepton $p_T > 15$ GeV and pseudorapidity $|\eta| < 1.1$ or $1.5 < |\eta| < 2.5$ for electrons and $|\eta| < 1.6$ for muons.

• Total vector sum $\vec{p}_T$ of neutrinos should be $> 20$ GeV (an approximate analog of missing $E_T > 20$ GeV in [18]).

• At least two jets are required with $p_T > 20$ GeV and $|\eta| < 2.5$. Jets are found by the D0 Run II midpoint cone algorithm with radius $R$=0.5 [19]. For this aim we used the FASTJET package [20] interfaced to PYTHIA 8.

• Scalar sum of the jet transverse momenta ($HT$) is required to be $HT > 60$ GeV for the 2 jet final state and $HT > 80$ GeV for the 3 jet one.

### B. Normalizations

The cross sections of the simulated events were normalized to either experimentally measured cross sections or to theoretical NNLO predictions. Specifically, we normalized all the PYTHIA cross sections in the following way:

• We simulated dijet events production and calculated cross sections in the dijet mass bins $150 - 175$ and $175 - 200$ GeV, and the two rapidity regions of $|y| < 0.4$ and $0.4 < |y| < 0.8$ available from the recent D0 measurement [21]. We have found that a required PYTHIA-to-data correction factor ("K-factor") is about 2.2 valid for both the dijet mass bins and the two rapidity regions.

• We also simulated separately the W inclusive production and from a comparison of its cross section with the D0 and CDF measurements [22] we have obtained the PYTHIA-to-data K-factor to be about 1.5.

• The $HW$ cross section was normalized to the NNLO predictions [23] with the PYTHIA-to-NNLO K-factor equal to 1.45.

• We corrected the effective cross section $\sigma_{\rm eff}$ used in Tune 2C [2] by a factor 1.6 to match to the CDF and D0 measurements [5, 8] with the averaged result $\sigma_{\rm eff}^{\rm ave} = 15.5$ mb.

The uncertainty assigned in the analysis to the first three K-factors are 10% and 16% to $\sigma_{\rm eff}^{\rm ave}$. The latter is caused by the difference between the D0 and CDF $\sigma_{\rm eff}$ central values ($\sim$7%) and the systematic uncertainties ($\sim$14%) in the D0 measurement.

## III. $d\sigma/dM_{jj}$ CROSS SECTIONS FOR $HW$ AND DOUBLE PARTON EVENTS

### A. HW and DP cross sections

In this section we calculate differential cross sections $d\sigma/dM_{jj}$ for the $HW$ and DP ($W$+dijet) events selected according to the criteria described in Section II. To be closer to real detector conditions, the jet transverse momenta are smeared with a detector $p_T$ resolution. Specifically, we smeared a jet $p_T$ according to:

$$\frac{\sigma_{p_T}}{p_T} = \frac{S}{\sqrt{p_T}} \oplus C, \tag{2}$$

where we take $S = 0.75$ and $C = 0.06$ which approximately reproduce the jet $p_T$ resolution numbers for the D0 detector [24]. The differential cross sections $d\sigma/dM_{jj}$ for the $HW$ and DP productions with account of the smearing effect are

[2] The effective cross section $\sigma_{\rm eff}$ in PYTHIA 8 is taken as a ratio of a total non-diffractive cross section to an impact-parameter enhancement factor, depending on the parton spatial density distribution.

shown in Fig. 2. In addition to the total DP cross section, contributions from main DP scattering subprocesses are also shown in an individual plot. One can see from these two plots that (a) the DP cross section is by more than two orders of magnitude dominates over the $HW$ signal, and (b) the DP cross section is mainly caused by the $W$+2 light jets (stemming from $u/d/s$-quarks or gluons) production, followed, in the order of importance, by contributions from $W + gc$ and $W + gb$, and then by $W + c\bar{c}$ and $W + b\bar{b}$ events.

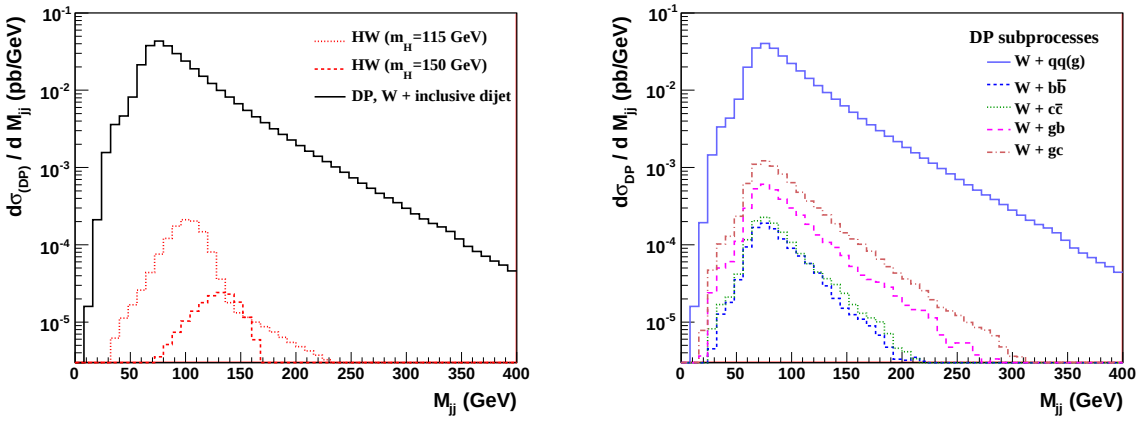


Figure 2: Differential cross sections in the dijet mass $M_{jj}$ bins for signal $HW$ and background DP events with account of the jet $p_T$ resolution. On the left plot, dotted and dash-dotted red lines correspond to $HW$ events with $m(H) = 115$ and 150 GeV while full black line shows the total background from all the DP $W$+dijet channels. The right plot shows contributions from main parton scattering subprocesses composing the total DP background.

### B. Account of $b$-jet identification efficiencies

The signal event final state is specified by a presence of two $b$-jets. Since the leading DP background is caused by the events with $W$+2 light jets in the final state (Fig. 2), we should expect its significant reduction after a requirement of jet $b$-tagging, especially double $b$-tagging. To check this numerically, we have to apply such a requirement for the $HW$ and DP events. In fast MC it is impossible to check a jet $b$-tagging quality, but the efficiencies to pass the $b$-tagging requirements for light ($l$), $c$ and $b$-jets from [25], parametrized as functions of jet $p_T$ and $\eta$ can be used instead. These efficiencies were used to re-weight events according to the jet flavors. Typical $b$-tagging efficiencies were found to be $50 - 70\%$ for $b$-jets, $8 - 12\%$ for $c$-jets and $0.5 - 2\%$ for $l$-jets. The variations reflect dependence on the jet $p_T, \eta$ and tightness of the $b$-tagging condition. A jet is considered to be a $b$-jet if it has a $b$-quark in the jet cone; if the jet does not have a $b$-quark but has a $c$-quark instead, it is considered to be a $c$-jet; otherwise it is a light jet. Fig. 3 shows cross sections multiplied by $b$-jet identification efficiency ($\varepsilon^{\rm jet}_{\rm b-id}$) for the DP and $HW$ events with double $b$-tagging applied, where each of the two jets is required to satisfy the "loose" requirement [25]. This requirement significantly suppresses rates of the DP events. However, the signal rates are also noticeably reduced (compare Figs. 2 and 3). For this reason, in practice, the double tagging is usually combined with a single tagging. For example, in the search for $HW$ signal [18], two cases of the $b$-tagging are considered: an event should contain either two jets satisfying "loose" $b$-tagging requirements or, if it fails, a single jet satisfying the "tight" requirement. Fractions of background (=data) and the $HW$ events selected with the single $b$-tagging can be taken from [18]: they are about 85% and 60% correspondingly[3]. The remaining events are with two $b$-tagged jets. Fig. 4 shows cross sections $\times\varepsilon^{\rm jet}_{\rm b-id}$ for the DP and HW events where we have combined events with single and double $b$-tagging with account of their fractions mentioned above. We see that while the dominating DP channel is still caused by the $W$+2 light jet production, the relative contribution from $W + gb$ production is now much higher than in Fig. 2 (no $b$-tagging is applied). The $W + gb$ contribution is followed by about similar ones from the $W + gc$ and $W + b\bar{b}$ events.

Fig. 5 is complementary to Fig. 4 and shows ratios of $HW$ to the inclusive DP $W$+dijet event yields in the bins of the dijet mass $M_{jj}$ for the events selected by the combined $b$-tagging. The uncertainty in each bin are caused by the K-factors and effective cross section (Section II). One can see that the Higgs boson signal with $m_H = 115$ GeV is expected to be suppressed by about a factor 5 ($S/B \simeq 0.2$) in the peak position, while the signal events with $m_H = 150$ GeV are suppressed by about a factor 12.

[3] Clearly, here we assume that the jet flavor content of the background events in data and the dijet events from the DP interaction is the same. However, we believe that for the current level of estimates this assumption should be good enough.

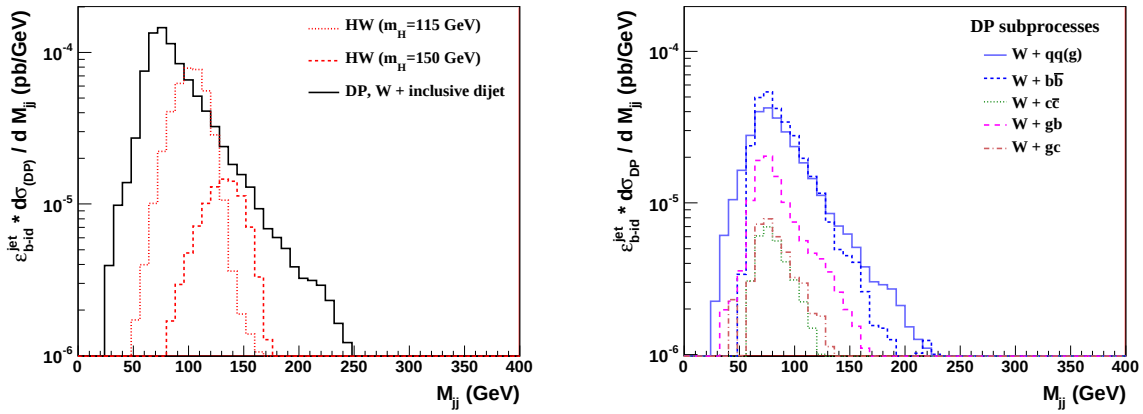


Figure 3: Differential cross sections in the dijet mass bins for signal $HW$ and background DP events with account of the jet $p_T$ resolution with double $b$-tagging (two "Loose") requirement. On the left plot, dotted and dash-dotted red lines correspond to $HW$ events with $m(H) = 115$ and 150 GeV while full black line shows the total background from all the DP $W$+dijet channels. Right plot demonstrates contributions from various subprocesses composing the total DP background.

It is interesting to compare the total number of the signal events predicted by fast MC after all selections (Fig. 4) with that in [18] for the integrated luminosity $L_{int} = 5.3$ fb$^{-1}$. It is obtained by integrating the cross section over the whole $M_{jj}$ range (20–400 GeV) and multiplying by $L_{int}$. In such a way we have found that expected signal statistics should be about 31 (7) events for $m_H = 115$ (150) GeV. According to [18] there should be selected about $19 \pm 1$ events for $m_H = 115$ GeV. Our estimate seems to be in a reasonable agreement if we take into account the effects of finite lepton identification, jet tagability efficiencies and detector acceptance unaccounted in our fast MC.

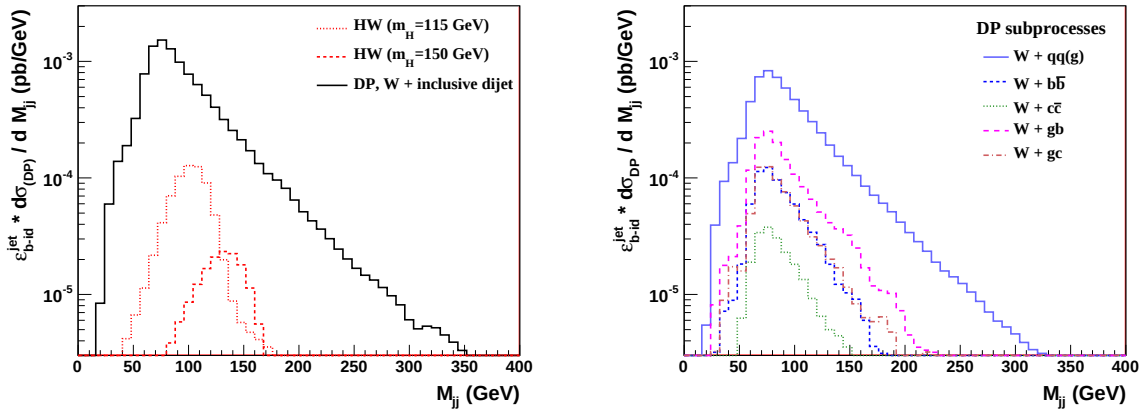


Figure 4: Differential cross sections in the dijet mass bins for signal HW and background DP events with account of the jet $p_T$ smearing and corrected for the jet $b$-tagging efficiency (see also description in the caption to Fig. 2).

## IV. COMPARISON OF DP AND SP EVENT YIELDS

In this section we compare the event yields $dN/dM_{jj}$ expected for the DP and SP $W$+2-jet productions. The two additional jets in the SP events are coming from radiation effects in initial and/or final states. To simulate SP events we used $q\bar{q} \to Wg$ and $qg \to Wq$ subprocesses and applied the $HW$ selection criteria from Section II. Also, as before, the jet $p_T$ was smeared according to the $p_T$ resolution [Eq.(2)] and the events were weighted with the jet $b$-tagging efficiencies according to the jet flavors.

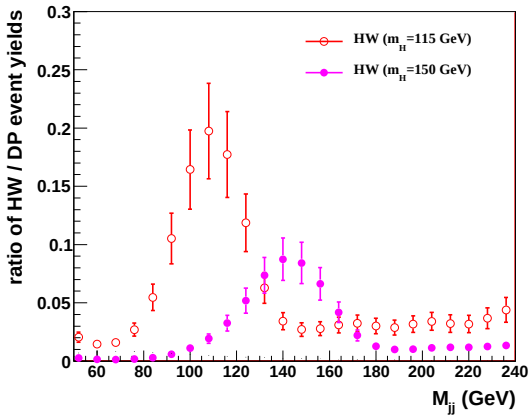


Figure 5: Ratio of $HW$ signal to DP background event yields with the combined $b$-tagging (see the main text).

The estimated total event yields in the whole mass region at $L_{int} = 5.3$ fb$^{-1}$ for SP and DP events are about 4105 and 460 events, correspondingly. The differential ratios of the DP/SP $W$+2-jet event yields in the $M_{jj}$ bins are shown in Fig. 6. They are about $12 - 14\%$ for $M_{jj} \simeq 115$ GeV and $9 - 11\%$ for $M_{jj} \simeq 150$ GeV. Thus, we see that the DP contribution is quite noticeable being compared with the traditional SP background to the $HW$ events. Such a level of the DP background is not surprising in the light of tendency for the DP fractions versus jet $p_T$ observed in the CDF and D0 measurements with $\gamma$+3 jet events [5, 8].

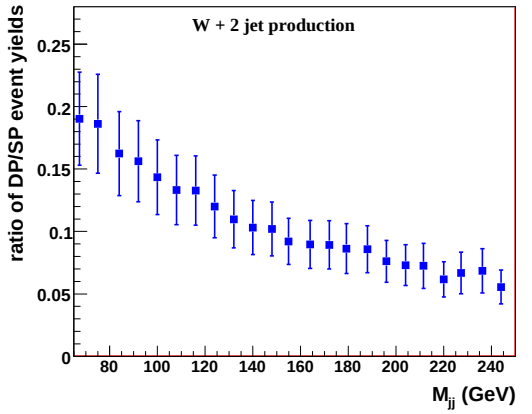


Figure 6: Ratio of DP to SP event yields for the $W$+2-jet production.

## V. ARTIFICIAL NEURAL NETWORK FOR SEPARATION OF DP AND $HW(Z)$ EVENTS

### A. Variables

In this section we discuss variables that can be useful to separate the $HW(Z)$ signal and the DP $W(Z)$+dijet background events. Most of these variables are either based on the previous relevant experimental studies [1–8] or have been suggested in theoretical papers [11, 26–30]. Due to a similarity of $HW$ and $HZ$ events, most of these variables should be useful to suppress the DP background events in both the final states (with some exclusions). Definitions of all the variables are summarized below.

• First variable is an azimuthal angle between two $p_T$ vectors, where the first one corresponds to $W(Z)$ $p_T$ vector, while the second one is a sum of the leading and second jet $p_T$ vectors:

$$\Delta S \equiv \Delta\phi\left(\vec{p}_T[V],\ \vec{p}_T[\mathrm{jet}_1, \mathrm{jet}_2]\right), \tag{3}$$

where $\vec{p}_T[V]$ is a transverse momentum vector of V(=W,Z)-boson and $\vec{p}_T[\mathrm{jet}_1, \mathrm{jet}_2] = \vec{p}_T^{\,\mathrm{jet}_1} + \vec{p}_T^{\,\mathrm{jet}_2}$. For historical reasons [1–5, 8] we call this angle as $\Delta S$.

• Second variable is a difference between rapidity of V-boson and total rapidity of the two-jet system:

$$\Delta\eta(\mathrm{V}, \mathrm{jet12}) = |\eta^{\mathrm{V}} - (\eta^{\mathrm{jet1}} + \eta^{\mathrm{jet2}})|. \tag{4}$$

• Certainly, variable $\Delta\eta(\mathrm{V}, \mathrm{jet12})$ can be calculated just for $V = Z$ events, but not for $W$ due to a missed $p_z$ information of $\nu$. Instead we can use a rapidity of the electron ($e$) $\eta^e$ from the $W$ decay and introduce analogous variable:

$$\Delta\eta(\mathrm{e}, \mathrm{jet12}) = |\eta^{e} - (\eta^{\mathrm{jet1}} + \eta^{\mathrm{jet2}})|. \tag{5}$$

• In case of the $W$ production one can also consider an azimuthal angle between electron from the $W$ decay and the leading jet $\Delta\phi(\mathrm{e}, \mathrm{jet1})$.

Two other variables are angular differences between the first and second jets:

• an azimuthal angle between the jets $\Delta\phi(\mathrm{jet1}, \mathrm{jet2})$.

• a difference between rapidities of the first and second jets $\Delta\eta(\mathrm{jet1}, \mathrm{jet2})$.

• Another variable characterizes orientation of the two event planes, where the first plane contains the beam (proton) axis and V-boson, and the second one contains the two jets [31]:

$$Cos\psi^{\star}(\mathrm{V}, \mathrm{jet12}) = \frac{(\vec{p}^{\,V} \times \vec{p}^{\,\mathrm{proton}}) \cdot (\vec{p}^{\,\mathrm{jet1}} \times \vec{p}^{\,\mathrm{jet2}})}{|\vec{p}^{\,V} \times \vec{p}^{\,\mathrm{proton}}| \cdot |\vec{p}^{\,\mathrm{jet1}} \times \vec{p}^{\,\mathrm{jet2}}|}. \tag{6}$$

• In case of the $W$ production, we do not have 3-vector of the $W$ momentum but can use the electron 3-vector instead, i.e. we should calculate $Cos\psi^{\star}(e, \mathrm{jet12})$.

Three other variables are based on the jet $p_T$:

• total sum of the first and second jet $p_T$:

$$p_T^{\mathrm{sum12}} = p_T^{\mathrm{jet1}} + p_T^{\mathrm{jet2}}. \tag{7}$$

• relative difference between the first and second jet $p_T$:

$$p_T^{\mathrm{diff12}} = (p_T^{\mathrm{jet1}} - p_T^{\mathrm{jet2}})/p_T^{\mathrm{sum12}}. \tag{8}$$

• total $p_T$ sum of all jets, $p_T^{\mathrm{sumAll}}$.

• Finally, we add the total number of all jets ($p_T > 6$ GeV), $N_{\mathrm{jets}}$.

All these 12 variables are shown in Figs. 7 and 8 for $HW$ and DP $W$+dijet events. They demonstrate a good separation power between the two event types.

### B. ANN

The variables presented above can be used as an input to a dedicated ANN to separate between the $HW$ and DP events. Variable $p_T^{\mathrm{sumAll}}$ is very correlated with $p_T^{\mathrm{sum12}}$, but the latter is a bit more sensitive to the signal/background difference. We do not use the dijet mass information to be less dependent on a specific Higgs boson mass region but rather concentrate on other more generic kinematic properties of the two event types.

With account of the remarks above, we have used following 9 variables to train the ANN: $\Delta S$, $\Delta\eta(\mathrm{e}, \mathrm{jet12})$, $\Delta\phi(\mathrm{e}, \mathrm{jet1})$, $\Delta\phi(\mathrm{jet1}, \mathrm{jet2})$, $\Delta\eta(\mathrm{jet1}, \mathrm{jet2})$, $Cos\psi^{\star}(e, jet12)$, $p_T^{\mathrm{sum12}}$, $p_T^{\mathrm{diff12}}$, and $N_{\mathrm{jets}}$. The package JETNET [32] has been used for this aim. The ANN is trained using the signal $HW$ (simulated with $m_H = 115$ GeV) and background DP events to produce a single output value equal to zero for the background and unity for the signal events. The DP background events for the training (and later for testing) purpose are selected around the Higgs boson $M_{jj}$ peak position taking all events with $\pm 2\sigma$ around the peak. We have trained ANN using by 200,000 the signal and background events and then tested using by 50,000 those that have not been used at the training stage. Normalized distributions of the signal and background events over the ANN output $O_{\mathrm{NN}}$ is presented in Fig. 9. The ANN, already obtained at the training stage, has been used later to also separate the $HW$ signal simulated with $m_H = 150$ GeV and DP events.

The tighter cut on the ANN output we apply the larger fraction of DP events can be rejected. Fig. 10 shows a correlation between efficiencies to select the background and signal events ($\varepsilon_b^{\rm ANN}$ and $\varepsilon_s^{\rm ANN}$, respectively) for the two Higgs boson masses, $m_H = 115$ GeV and $m_H = 150$ GeV. One can see that taking 90% (80%) of the signal events with $m_H = 115$ GeV we select only about 24% (13%) of the DP events, while taking 90% (80%) of the signal events with $m_H = 150$ GeV we have only about 9% (4%) of the DP events.

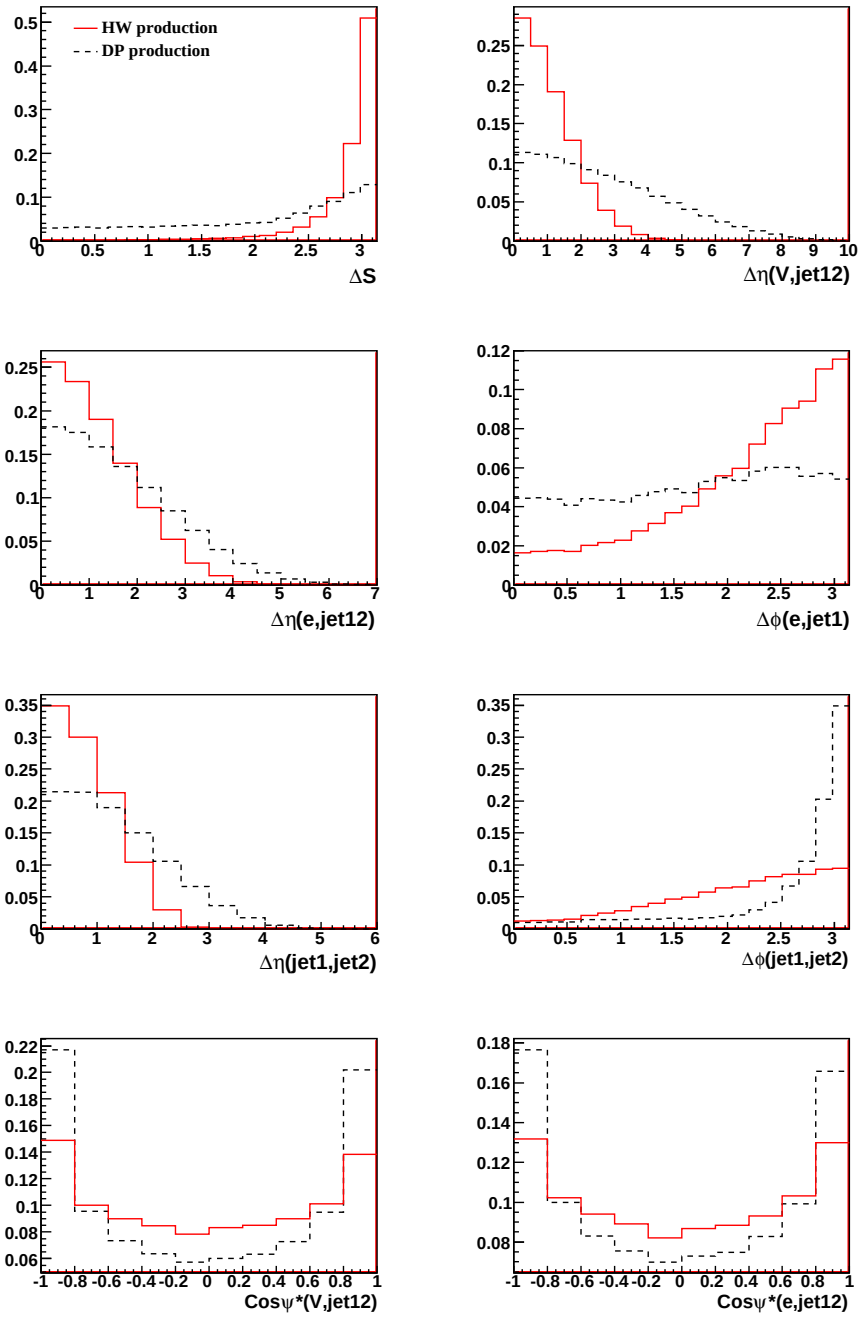


Figure 7: Normalized distributions of the number of $HW$ signal (full red line) and $W$+dijets background (dashed black line) events over the kinematic variables of Section V A (part 1).

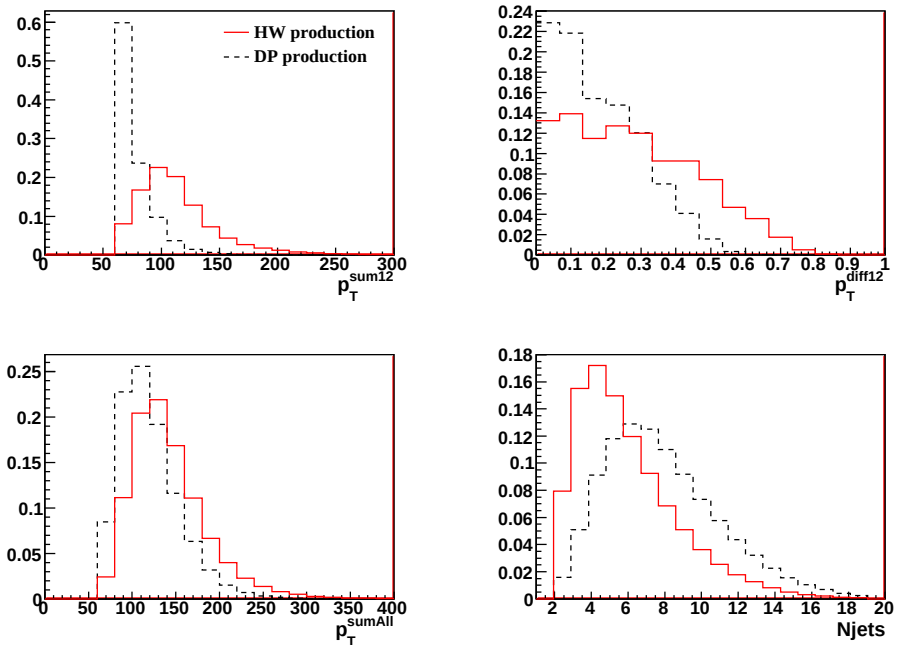


Figure 8: Normalized distributions of the number of $HW$ signal (full red line) and $W$+dijets background (dashed black line) events over the kinematic variables of Section V A (part 2).

### C. Results

The built ANN is used to further suppress the DP background, strongly dominating over the signal events even after the b-tagging selections (Fig. 5). The new signal-to-background ratios are shown in two plots of Fig. 11, corresponding to the choice of the $HW$ signal efficiencies $\varepsilon_s^{\rm ANN} = 90\%$ and 80%. One can see that the ratios at $\varepsilon_s^{\rm ANN} = 90\%$ for both the mass regions, 115 GeV and 150 GeV, are now close to $0.8 - 0.9$. This ratio is growing further with $\varepsilon_s^{\rm ANN} = 80\%$, and it reaches about 1.25 at $M_{jj} \simeq 115$ GeV and about 1.6 at $M_{jj} \simeq 150$ GeV.

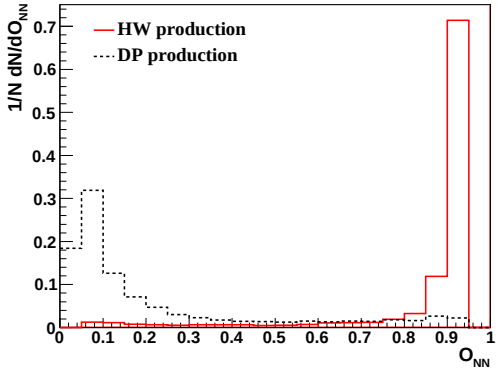


Figure 9: The ANN output for the DP and $HW$ ($m_H = 115$ GeV) events using the 9 input variables described in the text.

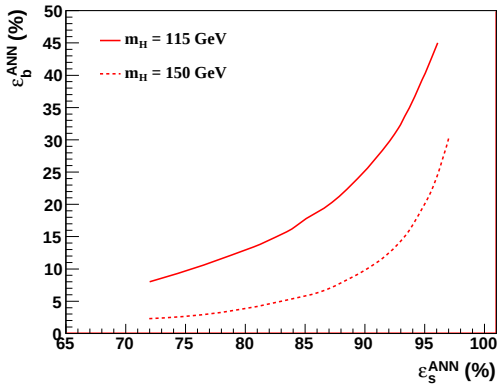


Figure 10: DP versus $HW$ neural network selection efficiencies.

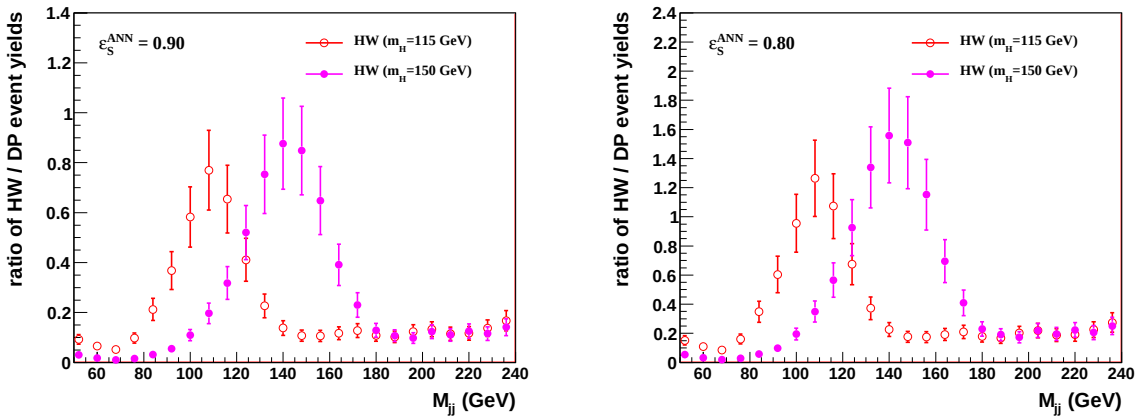


Figure 11: Ratio of the $HW$ event yields to the DP ones with account of the ANN selection efficiencies taken for the $HW$ events to be 90% on the left and 80% on the right plot.

## VI. CONCLUSION

In our current study we have shown that the $W$+dijet events produced due to the DP scattering can compose a quite sizable background to the associated $HW$ production with $H \to b\bar{b}$ decay. Its relative fraction with respect to the traditional background from SP scattering with the $W$+2-jet final state is found to be $9 - 13\%$ in the dijet mass region $115 < M_{jj} < 150$ GeV. We suggest a set of the angular and jet $p_T$ variables sensitive to the difference between the $HW$ and DP kinematics. The neural network built using these variables allows one to significantly suppress the DP background to a desirable level.


## Acknowledgments

The authors thank Wade Fisher and Aurelio Juste for quite useful discussions and Stephen Mrena for the help with using PYTHIA 8 code.

[1] T. Akesson *et al.* (AFS Collaboration), Z. Phys. C **34**, 163 (1987).
[2] C.E. Wulz, (UA1 Collaboration), Proc. of the 22nd Rencontres de Moriond, Les Arcs, France, 15-21 (1987).
[3] J. Alitti *et al.* (UA2 Collaboration), Phys. Lett. B **268**, 145 (1991).
[4] F. Abe *et al.* (CDF Collaboration), Phys. Rev. D **47**, 4857 (1993).
[5] F. Abe *et al.* (CDF Collaboration), Phys. Rev. D **56**, 3811 (1997).
[6] T. Alexopoulos *et al.* (E735 Collaboration), Phys. Lett. B **435**, 453 (1998).
[7] V.M. Abazov *et al.* (D0 Collaboration), Phys. Rev. D **67**, 052001 (2003).
[8] V.M. Abazov *et al.* (D0 Collaboration), Phys. Rev. D **81**, 052012 (2010).
[9] C. Gwenlan *et al.* (ZEUS Collaboration), Acta Phys. Polon. B **33**, 3123 (2002).
[10] F.D. Aaron *et al.* (H1 Collaboration), H1-prelim-08-036.
[11] T. Sjöstrand and M. van Zijl, Phys. Rev. D **36**, 2019 (1987).
[12] D. Fabbro, D. Treleani, Phys. Rev. D **61**, 077502 (2000); Phys. Rev. D **66**, 074012 (2002).
[13] M.Y. Hussein, Nucl. Phys. Proc. Suppl. **174**, 55 (2007).
[14] E.L. Berger, C.B. Jackson, G. Shaughnessy, Phys.Rev. D **81**, 014014 (2010).
[15] T. Sjöstrand *et al.*, JHEP **05**, 026 (2006); arXiv:0710.3820, http://home.thep.lu.se/ torbjorn/Pythia.html.
[16] T. Sjöstrand and P.Z. Scands, JHEP, **0403** (2004).
[17] This tune was suggested by the PYTHIA authors.
[18] V. Abazov *et al.* (D0 Collaboration), http://www-d0.fnal.gov/Run2Physics/WWW/results/prelim/HIGGS/H95/H95.pdf.
[19] G.C. Blazey *et al.*, arXiv:hep-ex/0005012 (2000).
[20] M. Cacciari and G.P. Salam, Phys.Lett. B**641**, 57 (2006).
[21] V. Abazov *et al.* (D0 Collaboration), Phys. Lett. B **693**, 531 (2010).
[22] V. Abazov *et al.* (D0 Collaboration), http://www-d0.fnal.gov/Run2Physics/WWW/results/prelim/EW/E06/E06.pdf; D. Acosta *et al.* (CDF Collaboration), Phys. Rev. Lett. **94**, 091803 (2005), hep-ex/0406078.
[23] T. Hahn *et al*, hep-ph/0607308.
[24] V. Abazov *et al.* (D0 Collaboration), Phys. Rev. Lett. **101**, 062001 (2008).
[25] V. Abazov *et al.* (D0 Collaboration), Nucl. Instrum. Methods in Phys. Res. Sect. A **620**, 490 (2010).
[26] P.V. Landshoff and J.C. Polkinghorne, Phys. Rev. D **18**, 3344 (1978).
[27] C. Goebel, F. Halzen, and D.M. Scott, Phys. Rev. D **22**, 2789 (1980).
[28] F. Takagi, Phys. Rev. Lett. **43**, 1296 (1979); N. Paver and D. Treleani, Nuovo Cimento A **70**, 215 (1982).
[29] B. Humpert, Phys. Lett. B **131**, 461 (1983); B. Humpert and R. Odorico, Phys. Lett. B **154**, 211 (1985).
[30] M.L. Mangano, Z. Phys. C **42**, 331 (1989).
[31] V.M. Abachi *et al.* (D0 Collaboration), Phys. Rev. D **53**, 6000 (1996).
[32] C. Peterson, T. Rognvaldsson, L. Lönblad, Comput. Phys. Commun. **81**, 15 (1994). 5
[33] G. Calucci and D. Treleani, Nucl. Phys. B (Proc. Suppl.) **71**, 392 (1999); Phys. Rev. D **60** (1999) 054023; Phys. Rev. D **79**, 074013 (2009).